9-1-1999

Evolution of the Lithium Abundances of Solar-Type Stars. IX. High-Resolution Spectroscopy of Low-Mass Stars in NGC 2264

David R. Soderblom
Space Telescope Science Institute

Jeremy R. King
Clemson University, jking2@clemson.edu

Lionel Siess
Space Telescope Science Institute

Burton F. Jones
University of California

Debra Fischer
San Francisco State University

THE ASTRONOMICAL JOURNAL, 118:1301–1314, 1999 September

EVOLUTION OF THE LITHIUM ABUNDANCES OF SOLAR-TYPE STARS. IX. HIGH-RESOLUTION SPECTROSCOPY OF LOW-MASS STARS IN NGC 2264

DAVID R. SODERBLOM, JEREMY R. KING, AND LIONEL SIESS
Space Telescope Science Institute, 3700 San Martin Drive, Baltimore, MD 21218; soderblom@stsci.edu, jking@stsci.edu, siess@stsci.edu
BURTON F. JONES
UCO/Lick Observatory, Board of Studies in Astronomy and Astrophysics, University of California, Santa Cruz, CA 95064; jones@ucolick.org
AND
DEBRA FISCHER
Department of Physics and Astronomy, San Francisco State University, San Francisco, CA 94132; fischer@stars.sfsu.edu
Received 1999 April 20; accepted 1999 June 4

ABSTRACT

We have obtained Keck HIRES spectra of 35 objects in the pre–main-sequence cluster NGC 2264 in order to determine their radial velocities, rotation rates, activity levels, and Li abundances. Our precise radial velocities indicate that the eight objects we observed that lie below a 5 Myr isochrone are nonmembers. This means that the age spread within NGC 2264 is only about 4 Myr, a factor of 2 less than found previously, although this is a lower limit to the true age spread because star formation is still taking place in the cluster. After correction for non-LTE effects, our Li abundances are consistent with no depletion having yet occurred and a uniform value of log N(Li) = 3.2, provided that the uncertainty in $T_{\rm eff}$ values is about 250 K. This is high, but this cluster appears to have varying extinction, which could lead to large temperature errors. Stars in NGC 2264 have spun up compared with the younger Orion Nebula cluster. Current models suggest disk-locking timescales of 1–2 Myr to account for the most rapidly rotating stars. By combining rotation periods and $v \sin i$ values, we show that the distribution of $\sin i$ is not in accord with a random distribution of rotation axes. The reason for this is not known, but it is probably due to a selection against equator-on objects that still have obscuring material around them.

Key words: color-magnitude diagrams — open clusters and associations: individual (NGC 2264) — stars: abundances — stars: activity — stars: evolution — stars: rotation

1. THE PRE–MAIN-SEQUENCE PHASE FOR SOLAR-TYPE STARS

For a decade now we have presented and discussed results from high-resolution spectroscopy of solar-type stars in nearby open clusters. These data have been applied to the understanding of angular momentum loss and the relation between rotation and stellar activity (see, e.g., Soderblom et al. 1993d, hereafter SSHJ; Soderblom et al. 1993e). However, most of our effort has been directed at the problem of lithium depletion in stars like the Sun. Li is destroyed in stellar interiors at temperatures above about 2.5 MK. This makes Li a useful tracer of processes related to convection, because the temperature at the base of the convective envelope in solar-type stars is very close to 2.5 MK. Clusters are natural targets of study because they provide reasonably sized samples of stars of known age and composition and because they allow us to construct an evolutionary sequence. Table 1 summarizes the cluster observations of Li that have been made.

During pre–main-sequence contraction, low-mass stars ($M < 1\ M_\odot$) should undergo significant depletion of Li in their outer envelope as the temperature at the base of the convective zone becomes hot enough to burn Li. Standard models (with no rotation or diffusion) indicate that the depletion should be an increasing function of decreasing stellar mass and should depend only on mass and metallicity.

Cluster observations are now extensive enough that they cannot be recapitulated briefly. Each cluster has its own story to tell, because each one has a different age and composition, different stellar content, and perhaps different initial conditions as well. As the sample grows, we can hope to learn how much clusters differ from one another simply because of the consequences of initial conditions rather than processes that are part of stellar evolution. Discerning these differences among trends is difficult, because sometimes clusters are sparse, sometimes conditions prevent acquiring data for large samples, and sometimes the observations are of uneven quality. The increasing reach of new-generation telescopes is steadily remedying this situation.

Of all the clusters studied, the Pleiades stands out as the most interesting to us. At an age of 100 Myr, its solar-type stars have just recently reached the zero-age main sequence (ZAMS), meaning that many members maintain much of their initial angular momentum and are young enough that no main-sequence Li depletion should have taken place. The Pleiades is rich in members compared with most open clusters, and its membership is well studied, with highly probable members known into the brown dwarf regime.

The story that the Pleiades tells is fascinating. At 1 $M_\odot$ and below, its members have rotation rates spanning nearly 2 orders of magnitude. If the Hyades and Pleiades represent an evolutionary sequence, then this spread in rotation virtually disappears within 0.5 Gyr (Soderblom et al. 1993e). At a single mass, the Pleiades exhibits a spread in Li of a factor of about 30 (1.5 dex). Although this large spread is still not well understood, the general trend of depletion is in agreement with theoretical predictions. Although not as large as the spread in rotation, we view the spread in Li as more remarkable. This is because stars form with different

TABLE 1

OBSERVATIONS OF LITHIUM IN SOLAR-TYPE STARS IN OPEN CLUSTERS

Cluster	Age (Myr)	$m-M$	[Fe/H]	$E(B-V)$	N_{stars}	$B-V$ Range	Li References
Orion Ic	10:	8.7	−0.2	0.05	60	0.5–1.4	1–3
NGC 2264	10	9.4	−0.15	0.06	12	0.5–1.3	4
IC 2602	10	6.0	−0.20	0.04	24	0.4–1.4	5
IC 2391	36	5.7	−0.04	0.01	10	0.6–1.4	6
IC 4665	40	8.2	...	0.17	14	0.8–1.6	7
α Persei	50	6.4	+0.1	0.09	41	0.4–1.0	8–10
Blanco 1	50	6.4	+0.03	0.02	15	0.4–1.0	11
Pleiades	100	5.5	+0.11	0.04	100	0.4–1.4	8–15
NGC 2516	150	7.9	−0.32	0.12	33	0.6–1.0	16
M34 (NGC 1039)	200	8.2	−0.26	0.11	50	0.4–1.1	17
M7 (NGC 6475)	220	6.9	+0.1	0.06	37	0.5–1.1	18
UMa group	300	1.7	−0.08	0.00	15	0.4–1.0	19
Hyades	660	3.4	+0.12	0.00	70	0.4–0.8	20–25
Praesepe	660	5.5	+0.12	0.00	63	0.4–0.8	26
NGC 6633	660	7.5	−0.11	0.17	23	0.3–1.0	27
NGC 752	1100	8.0	−0.21	0.03	19	0.4–0.9	28, 29
M67 (NGC 2682)	4000	9.3	−0.10	0.08	46	0.5–0.7	30–34
NGC 188	5000	11.0	−0.06	0.08	8	0.7–1.1	29, 35

NOTE.—The information in the second through fifth columns is taken from Lang 1992. Cameron 1985 and Meynet, Mermilliod, & Maeder 1993 also present comprehensive data for clusters. These are meant to be only indicative, not definitive.

REFERENCES.—(1) King 1993; (2) Cunha et al. 1995; (3) Duncan & Rebull 1996; (4) King 1993; (5) Randich et al. 1997; (6) Stauffer et al. 1989; (7) Martín & Montes 1997; (8) Boesgaard, Budge, & Ramsay 1988; (9) Balachandran, Lambert, & Stauffer 1988; (10) Randich et al 1998; (11) Panagi et al. 1994; (12) Paper III; (13) García López et al. 1994; (14) Russell 1996; (15) Paper VI; (16) Jeffries, James, & Thurston 1998; (17) Paper VII; (18) James & Jeffries 1997; (19) Soderblom et al. 1993c (Paper II); (20) Cayrel et al. 1984; (21) Boesgaard & Tripicco 1986; (22) Boesgaard & Budge 1988; (23) Soderblom et al. 1990 (Paper I); (24) Thorburn et al. 1993; (25) Soderblom et al. 1995 (Paper V); (26) Soderblom et al. 1993a (Paper IV); (27) Jeffries 1997; (28) Hobbs & Pilachowski 1986a; (29) Pilachowski & Hobbs 1988; (30) Hobbs & Pilachowski 1986b; (31) Spite et al. 1987; (32) García López et al. 1988; (33) Pasquini, Randich, & Pallavincini 1997; (34) Jones, Fischer, & Soderblom 1999 (Paper VIII); (35) Hobbs & Pilachowski 1988.

angular momenta, yet we commonly assume that stars in a cluster all start with the same elemental abundances. How then, and when, does the spread in Li abundance at a single mass arise?

The early Pleiades observations (Soderblom et al. 1993b, hereafter Paper III) showed a correlation between excess Li and excess rotation for stars $\lesssim 1\ M_{\odot}$. More recent observations (Jones et al. 1996, hereafter Paper VI; García López et al. 1994) indicate that this correlation disappears for the lowest mass stars observed. These observations suggest that there may be some rotationally induced mechanisms that act to accelerate (or retard) Li depletion. If such a rotational mechanism exists, it seems likely to be related to the major structural changes and rapid spin-up that occur during a star's final approach to the ZAMS, and not related to suggested rotationally induced main-sequence Li depletion, which acts on a much longer timescale (see, e.g., Chaboyer, Demarque, & Pinsonneault 1995). Thus, we are led to explore the pre–main-sequence phase of stellar evolution in order to see what happens to stars even earlier in their lives.

All of the clusters in Table 1 are fairly old, so that their solar-type stars are on the main sequence, but it is now clear that what we see on the ZAMS is the result of what happened much earlier. Younger-than-ZAMS clusters are more difficult to study because their faint, low-mass members have often not been identified. However, recent work has tabulated members for the pre–main-sequence (PMS) cluster NGC 2264. This cluster is about 5 Myr old, much younger than even the youngest ZAMS clusters (which are 30–50 Myr old). Although star formation is still going on in NGC 2264 (Margulis, Lada, & Young 1989), it contains stars that are at least 5 Myr old. This is older than most T Tauri stars, which are 1–3 Myr old.

Here we report on observations we have obtained for low-mass stars in NGC 2264 and how these fit into the scheme of the evolution of solar-type stars. As with the main-sequence clusters, NGC 2264 challenges our understanding of stellar physics by adding complexity to the picture.

2. OBSERVATIONS AND DATA REDUCTION

2.1. *Sample Selection and Spectroscopy*

Several membership studies of NGC 2264 have been done over the years, based on photometry and astrometry and, more recently, Hα emission. The present sample was drawn from the astrometric study of Jones (1999). We chose stars near the center of the cluster to reduce the likelihood of observing nonmembers, although a more thorough coverage of the entire region needs to be done.

The stars observed are listed in Table 2. The identifications are J (Jones 1999), V (Vasilevskis, Sanders, & Balz 1965), W (Walker 1956), and S (Sung, Bessell, & Lee 1997). We will use the Jones numbers for reference in this paper.

Our spectra were obtained with the HIRES spectrograph (Vogt 1992) on the Keck I Telescope in 1998 January. We used the C1 entrance decker, which yields a projected slit width of 0.″86 (about 3 pixels) and a spectroscopic resolving power of about 45,000. The detector was a Tektronix 2048 × 2048 CCD with 24 × 24 μm pixels. Sixteen echelle

TABLE 2

JOURNAL OF OBSERVATIONS

IDENTIFICATION				HJD	EXPOSURE	S/N	PROBABILITY	v_{rad}	$v \sin i$		
J	V	W	S	(2,450,000+)	(s)	(pixel^{-1})	(%)	(km s^{-1})	(km s^{-1})	MEMBER?	NOTES
(1)	(2)	(3)	(4)	(5)	(6)	(7)	(8)	(9)	(10)	(11)	(12)
Probable Members											
236.....	...	...	64	823.02089	1800	39	97	+11.9	22	Y?	SB2?
277.....	...	...	78	823.00483	1200	49	97	+19.3	16	Y	SB2?
289.....	...	...	79	823.04624	1800	25	94	+23.4	8	Y	
334.....	...	...	88	822.77914	1200	37	95	+24.1	12	Y	
407.....	40	54	104	821.75863	1800	60	96	+24.5	4	Y	
428.....	...	...	108	821.78167	2400	50	85	+18.9	8	Y	
455.....	...	...	118	823.11127	1800	26	98	+20.3	18	Y	
538.....	...	...	135	822.81177	1800	37	93	+19.8	9	Y	
600.....	...	...	153	822.92265	1800	41	96	+20.6	6	Y	
606.....	55	...	157	822.94611	900	73	93	+29.9	13	Y?	SB2?
680.....	...	...	172	822.84772	1200	45	97	+20.0	6	Y	
682.....	...	...	175	822.79562	1200	51	83	+2.9	6	Y?	SB1?
755.....	...	...	190	821.90125	1200	31	97	+21.4	8	Y	
803.....	...	...	203	821.93356	1200	49	97	+21.8	7	Y	
824.....	80	110	208	821.94962	1200	51	96	+23.1	12	Y	
861.....	...	...	222	822.98186	1800	33	97	+21.9	8	Y	Asymm. CCF?
943A.....	...	134	249	822.77000	600	105	...	−1.0	12	Y	SB2
943B.....	...	134	249	822.77000	600	105	...	+41.6	13	Y	SB2
968.....	...	...	258	821.96571	1200	35	95	+22.4	6	Y	
971.....	96	...	259	822.83505	900	51	97	+18.7	11	Y	Asymm. CCF?
1017	112	...	285	822.07455	1200	54	97	+20.2	11	Y	Asymm. CCF?
1036	...	...	295	823.09479	1200	36	98	−34.1	18	Y?	SB2+?
1037	...	...	294	822.89635	1800	35	97	+15.6	11	Y?	SB1?
1077	126	169	309	823.06932	900	73	98	+0.7	7	Y?	SB1? 2?
1122	137	184	327	822.01405	1200	73	95	+20.8	15	Y	
				822.76083	600	45	95	+21.2	...	...	Asymm. CCF?
1146	143	...	339	822.06105	900	65	81	+16.9	32	Y?	Asymm. CCF?
1185	157	...	355	821.98180	1200	46	94	+16.3	15	Y?	Possible SB2
1197	161	...	359	821.99793	1200	39	95	+19.5	6	Y	
Nonmembers											
442.....	...	...	...	821.82308	2400	23	95	...	...	N?	DIBs
542.....	...	71	138	822.95881	1800	27	95	...	...	N?	DIBs
611.....	56	...	159	821.85334	1200	40	83	−15.5	4	N	
641.....	...	...	...	821.86949	2400	16	87	...	...	N?	DIBs
779.....	...	...	197	821.91746	1200	37	80	+7.6	5	N	
1088	128	...	313	823.08190	900	75	95	+7.1	2.5	N?	Or SB1?
1302	...	...	...	822.86629	2400	23	96	...	...	N?	DIBs
1328	...	...	385	822.03054	2400	31	93	...	...	N?	DIBs
				822.09089	2400	29	93	...	...	...	DIBs

orders were recorded from 6300 to 8730 Å. The full free spectral range did not fit on the CCD, but the spectra include Hα, the Li doublet at 6708 Å, and part of the Ca II infrared triplet (IRT) region. Exposure times (col. [6] of Table 2) ranged from 10 to 40 minutes and resulted in per-pixel signal-to-noise ratios (S/Ns) of 15–75.

The observations were reduced using routines in the ECHELLE package of IRAF.[1] We debiased the images, flat-fielded them, removed scattered light and background, extracted the individual orders, and applied wavelength calibrations (using an exposure of a ThAr lamp). Figure 1 shows our spectra at Li, Hα, and the 8662 Å line of the IRT.

[1] IRAF is distributed by the National Optical Astronomy Observatories, operated by the Association of Universities for Research in Astronomy, Inc., under cooperative agreement with the National Science Foundation.

2.2. *Radial Velocities*

We determined radial velocities (v_{rad}) from our spectra using a cross-correlation analysis carried out with the FXCOR routine in the IRAF RV package. Our afternoon sky spectrum was used as a solar-proxy template, and it also defined the zero point. We compared measured solar wavelengths with laboratory values; the differences indicate that our zero-point uncertainty is approximately 1.2 km s^{-1}.

The cross-correlations were performed using spectra from 6420 to 6500 Å. Small shifts between spectra were removed by determining corrections using the telluric *B*-band region (6866–6880 Å). The internal uncertainty in v_{rad} is typically 0.3–0.4 km s^{-1} and arises from random errors, the effects of filtering, and choice of fitting function. The final v_{rad} values (heliocentric) are listed in column (9) of Table 2.

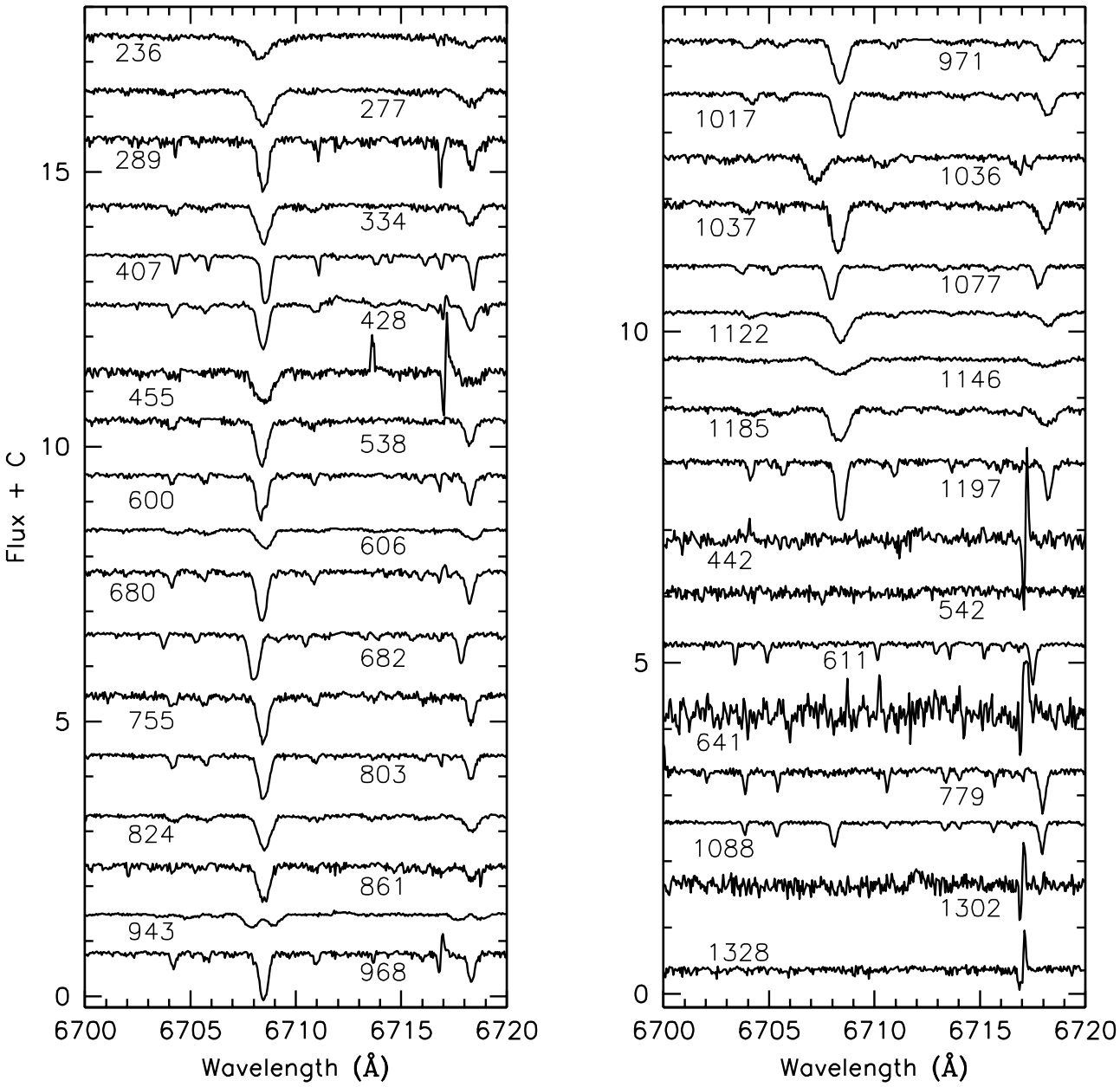

FIG. 1*a*

FIG. 1.—Keck HIRES spectra of the stars observed. Portions of the echelle spectra are shown at (*a*) the Li 6708 Å feature and (*b*, *c*) Hα and the 8662 Å line of the Ca II IRT. The emission-line spectra are ordered by decreasing strength of Hα strength, while the Li spectra are in the order stars are listed in Table 2. There is significant nebular Hα emission in NGC 2264, and it could not be completely removed. The dashed portions of the Hα profiles are affected by the imperfect subtraction and should be ignored.

Five of our stars (J442, J542, J641, J1302, and J1328) have nearly featureless spectra, making it impossible to determine $v_{\rm rad}$. Their Hα absorption wings are very broad, and the IRT lines are also broad and shallow. There is a narrow group of features present in all five of these spectra near 6614.3 Å, which we identify with the 6613.6 Å diffuse interstellar band (DIB) of Herbig & Leka (1991). We were also able to see other DIBs near 7224 and 7927 Å and, possibly, 8621 and 8649 Å. Other DIBs are expected to be too weak to be detected in our spectra. These stars are very red and are probably highly reddened background objects of early spectral type.

J943 (W134) was identified as a double-lined spectroscopic binary (SB2) by Padgett & Stapelfeldt (1994). In our spectrum the components are blended. We were able to measure $v_{\rm rad}$ for both components, but their Hα profiles are blended. The photometry is for both components together.

The median $v_{\rm rad}$ of the stars we believe to be probable members (see below) is $+20 \pm 3$ km s^{-1}. The median is less sensitive to outliers than an average, and we note that there is a significant low-velocity tail to the distribution because of multiples or contamination by nonmembers (Fig. 2). For the 18 most likely members, $\langle v_{\rm rad} \rangle = +21.2 \pm 1.8$ km s^{-1}. This is in good agreement with the values of Liu, Janes, & Bania (1989) and King (1993) for hotter members ($+24$ km s^{-1}).

2.3. *Rotation Rates and Multiplicity*

We used the same cross-correlations just described to determine rotation rates. The FWHM of the cross-

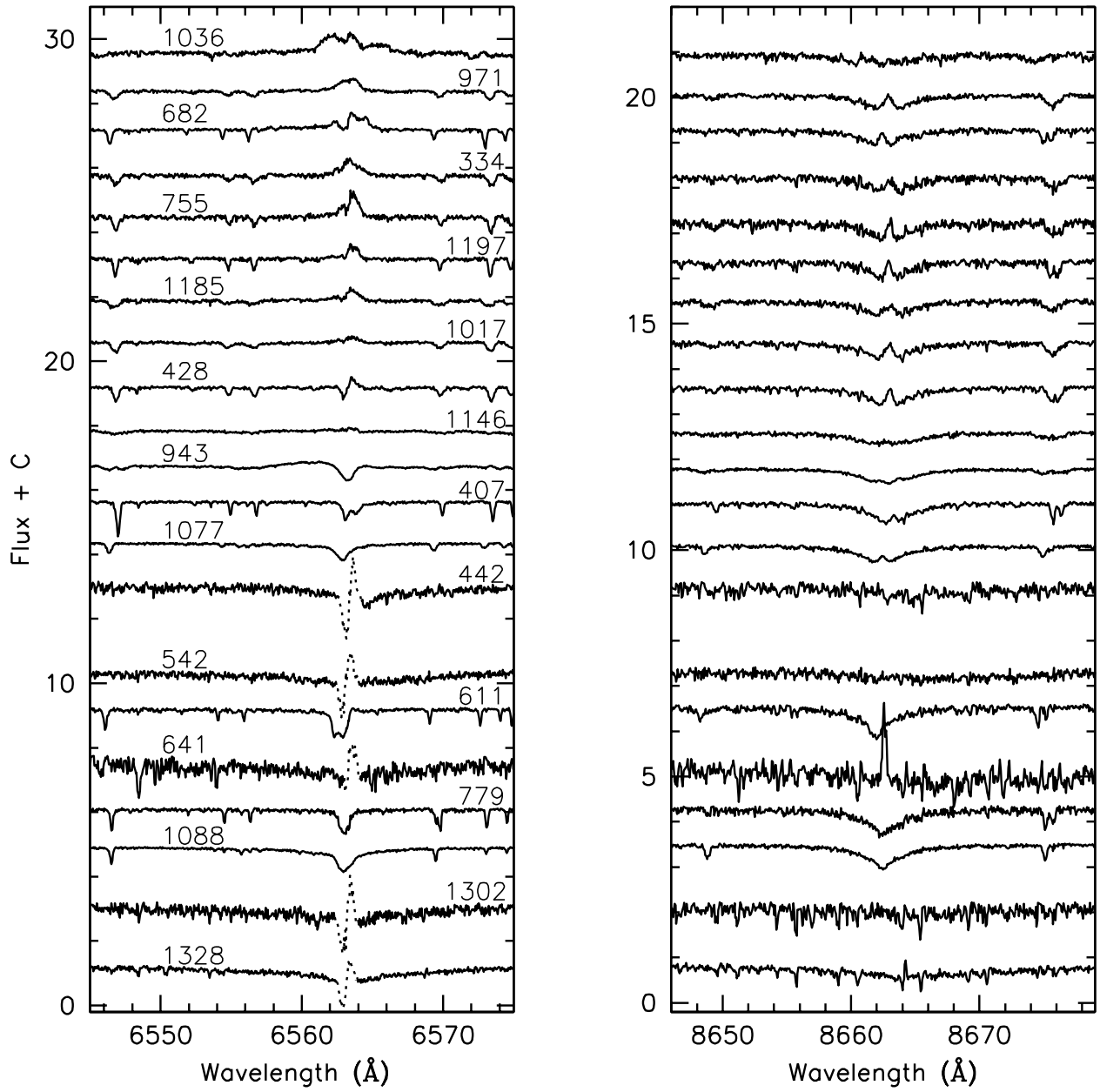

FIG. 1*b*

correlation function (CCF) was measured, and the relation of this quantity to rotation was mapped by convolving our solar spectrum with a rotational broadening function. Different $v \sin i$ values produced different templates, which were correlated with the solar spectrum. FWHM values were then measured to calibrate the relation.

The derived $v \sin i$ values are listed in column (10) of Table 2. There is a 2 km s^{-1} uncertainty for these values, estimated by comparing the different templates with the observed CCFs. We could not determine $v \sin i$ for the five featureless spectra.

Our spectra have good S/N, but these stars are not sharp-lined, and we did not obtain multiple spectra. Therefore, we cannot identify multiple systems with certainty. We have noted in the last column of Table 2 those cases where we suspect multiple components or where the CCF is asymmetric. SB2 indicates a double-lined spectroscopic binary, and SB1 stands for a single-lined spectroscopic binary. In some of these cases our $v \sin i$ values will turn out to be too large, because some of the line broadening is due to multiplicity. The accuracy of our $v_{\rm rad}$ values is affected by this as well.

3. DATA ANALYSIS

3.1. *Cluster Photometry*

We had available the photometric data of Sung et al. (1997, hereafter SBL) and R. Makidon (1997, private communication), as well as the photographic photometry of Jones (1999). We have taken $E(B-V) = 0.071$ and $A_V = 0.22$ (SBL). A distance modulus of 9.4 was used (SBL), corresponding to 760 pc. This modulus is much less than the 9.88 value determined by Pérez, Thé, & Westerlund (1987) but is close to the average of the many other determinations (9.31 mag) reported in Pérez et al.

The different colors are compared in Figure 3, where one

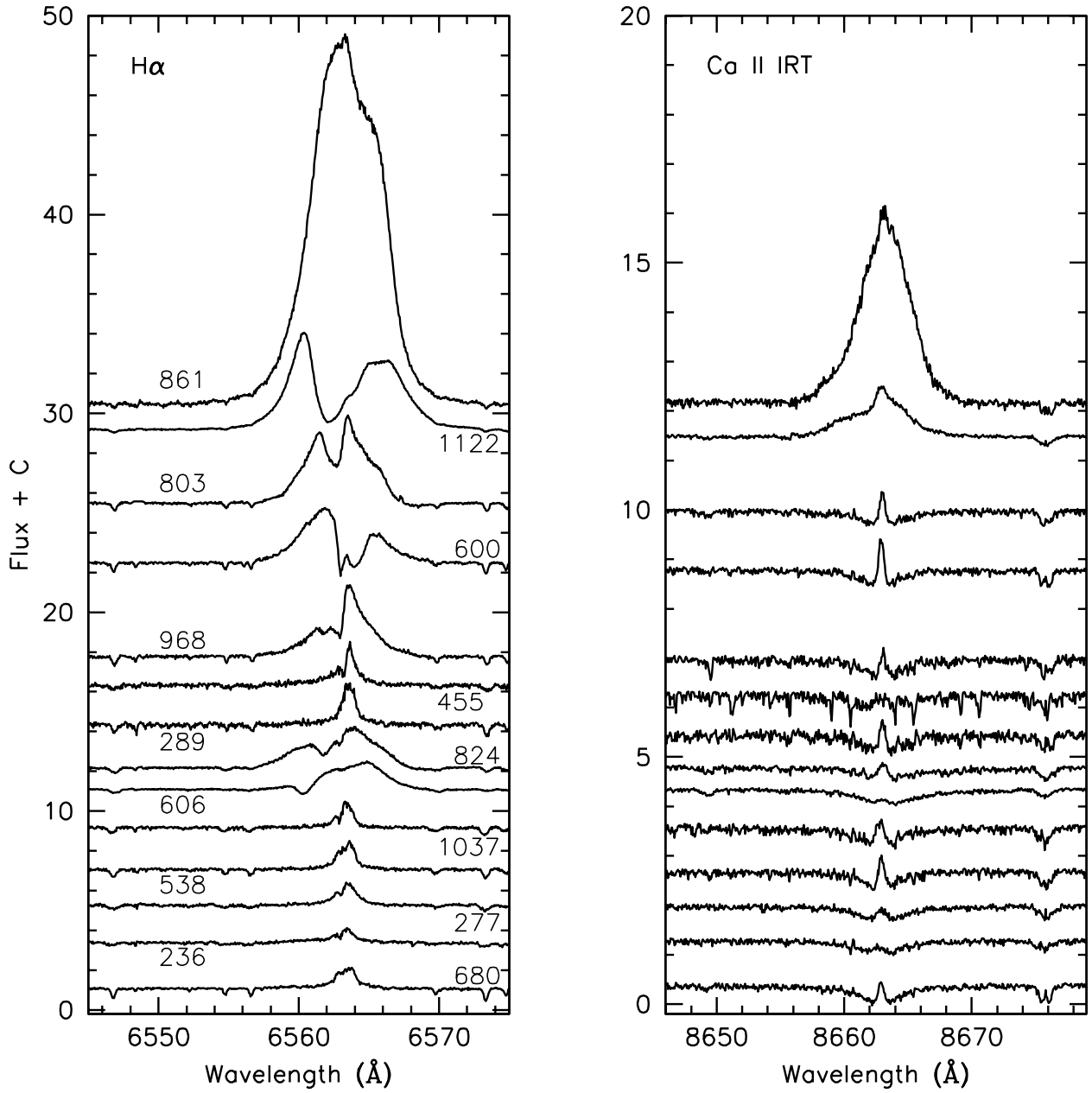

FIG. 1*c*

can see that $V-I$ colors[2] for most stars agree to within about 0.03 mag and m_V values agree to within about 0.05 mag. A few large discrepancies exist for a few stars. For consistency, we have used the photometry of SBL, but we note cases with discrepant photometry when that is pertinent. The measured $B-V$ colors are much less consistent, showing scatter of nearly 0.10 mag.

3.2. *Temperatures*

The determination of effective temperature ($T_{\rm eff}$) values for PMS stars is problematic (King 1998). The observational quantities used to infer $T_{\rm eff}$ have larger uncertainties than those for main-sequence stars because of reddening, extinction, and possible contributions from nonphotospheric emission. The interpretation of the colors or spectral types is also not straightforward. For example, different analyses of Li in PMS stars have used substantially different $T_{\rm eff}$ values, leading to very different Li abundances, and temperatures inferred from spectral types may have significant errors (Padgett 1996; King 1993). $T_{\rm eff}$ may also be determined from a fine analysis of many absorption lines over a range of wavelengths, but inadequate correction for spectral veiling can skew the results.

We used both $B-V$ and $V-I$ to determine $T_{\rm eff}$. The color-temperature calibrations are those of Bessell (1979), expressed in terms of $B-V$ by SSHJ and in terms of $V-I$ by Randich et al. (1997). Doing this makes our $T_{\rm eff}$ scale consistent with those used for the Pleiades (Paper III) and IC 2602 (Randich et al. 1997), as well as for other main-sequence clusters. As noted, we corrected the SBL colors for reddening of $E(B-V)=0.071$ and $E(V-I)/E(B-V)=1.31$.

[2] We have assumed that SBL's *I*-band measurements use the Cousins filter because Bessell is one of that study's authors, but SBL do not state this explicitly.

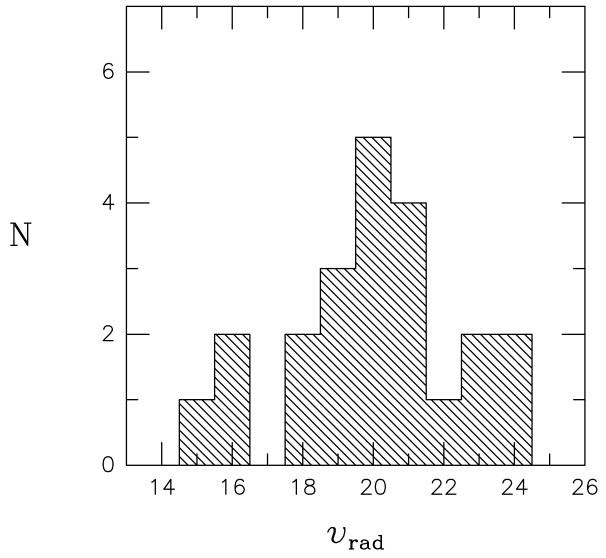

FIG. 2.—Distribution of v_{rad}. Only those values near the cluster mean are shown. The average is about 20 km s^{-1}.

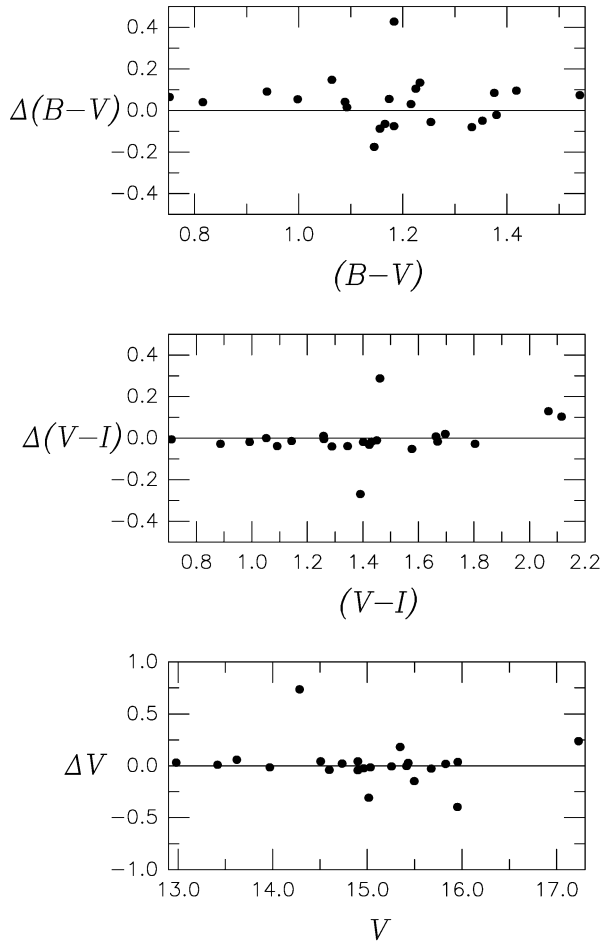

FIG. 3.—Comparison of the photometry of Sung et al. (1997) and Makidon et al. (1997). In each case the quantity plotted is Makidon's value minus Sung's value, with the abscissa showing Makidon's results. The $V-I$ values agree especially well for most stars. One star, J1122, is responsible for the most deviant point in each panel, and it probably represents a misidentification by one of the authors.

The dereddened colors are listed in columns (3) and (4) of Table 3. We also list colors for the five background stars mentioned earlier, although additional reddening corrections may be needed. For three of these latter objects, $V-I$ was taken from R. Makidon (1997, private communication).

Before comparing the T_{eff} values derived from $B-V$ and $V-I$, we chose to ignore these stars: the five heavily reddened background objects, J943 (as an SB2), and J611 and J779, because they appear to be nonmembers based on v_{rad} proper motion, Li, and Hα. The difference between T_{eff} values from the two color indexes is shown in Figure 4. $B-V$ consistently leads to T_{eff} values about 200 K hotter than $V-I$ does. We suspect that this may be due to boundary-layer emission that raises the blue flux. Similar color-dependent T_{eff} differences have been noted in IC 2602 (Randich et al. 1997, their Fig. 3) and also for the Pleiades and α Persei clusters (García López, Rebolo, & Martín 1994).

Some stars have differences in T_{eff} of 200–1000 K. Several have Hα emission and $R-I$ colors that are consistent with $V-I$ but not with $B-V$. The boundary-layer emission hypothesis means that the $V-I$ color should be a more reliable temperature indicator than $B-V$, especially when Hα emission is strong. Thus, we used only $V-I$ to derive T_{eff} for 12 of the stars with strong Hα emission, and we used both $V-I$ and $B-V$ for the remainder. When only $V-I$ was used, we added 37 K to the derived value to get agreement between the $V-I$ and $B-V$ derived temperature scales for the stars where both were used. Our T_{eff} values are in column (5) of Table 3. We have also included in Table 3 our derived estimates of masses and radii.

3.3. *Lithium Abundances*

We measured the strength of the Li 6708 Å doublet using both profile fitting and simple integration. The Li feature is strong in these stars and so is generally blended with the Fe I line at 6707.441 Å; correction for this blend was made using the parameterization in Paper III, and these correc-

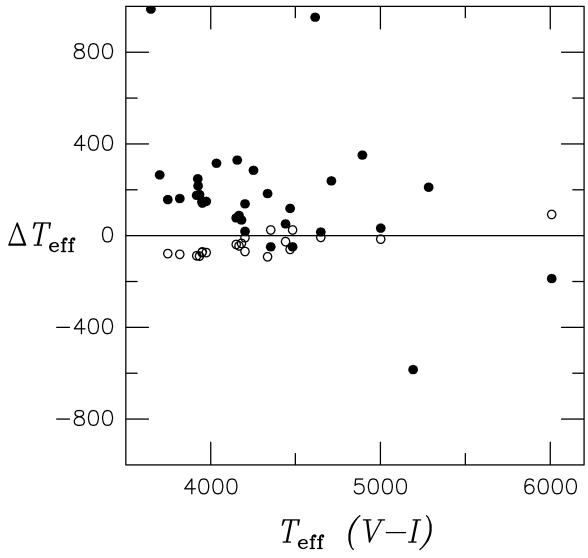

FIG. 4.—Comparison of T_{eff} values. The abscissa is T_{eff} as determined from $(V-I)_0$. The filled circles show $\Delta T_{eff} = T_{eff}(B-V) - T_{eff}(V-I)$, so that $(B-V)_0$ predicts a T_{eff} value that is typically about 200 K hotter than $(V-I)_0$ does. The open circles are T_{eff} from Sung et al. (1997) minus T_{eff} from $(V-I)_0$.

TABLE 3

NGC 2264 Li Abundances

Star (1)	W_λ(Hα) (Å) (2)	$(B-V)_0$ (3)	$(V-I)_0$ (4)	$T_{\rm eff}$ (K) (5)	M ($M_\odot$) (6)	R ($R_\odot$) (7)	W_λ(Li) (mÅ) (8)	$W_\lambda^{\rm corr}$(Li) (mÅ) (9)	log N(Li) LTE (10)	log N(Li) Non-LTE (11)
Probable Members										
J236.....	1.8	1.133	1.223	4330	0.93	1.74	663	682	3.53	3.45
J277.....	2.0	1.395	1.847	3826	0.29	2.39	690	705	3.03:	2.93:
J289.....	2.6	1.342	1.920	3833:	0.31	1.39	556	569	2.78:	2.72:
J334.....	0.6	1.176	1.327	4213	0.85	1.38	532	527	3.04	2.94
J407.....	Abs.	1.072	1.148	4459	1.05	2.07	493	474	3.22	3.12
J428.....	0.1	1.162	1.343	4216	0.78	1.63	497	476	2.89	2.81
J455.....	3.1	1.330	1.739	3899	0.38	2.06	642	670	3.04:	2.94:
J538.....	1.8	1.252	1.604	4005	0.56	1.42	550	558	2.92	2.83
J600.....	11.7	1.239	1.584	3971	0.55	1.60	509	587	2.95	2.86
J606.....	6.3	0.778	0.959	4931:	1.60	2.34	294	314	3.11:	2.92:
J680.....	1.7	1.250	1.567	4022	0.52	2.03	551	558	2.94	2.85
J682.....	0.8	1.233	1.537	4048	0.54	2.29	508	502	2.82	2.74
J755.....	0.6	1.173	1.368	4190	0.82	1.33	543	537	3.04	2.95
J803.....	19.4	1.159	1.355	4204	0.72	1.95	504	626	3.26	3.17
J824.....	10.6	1.036	1.236	4371	0.85	2.15	465	534	3.27	3.17
J861.....	122.2	0.988	2.002	3684:	0.24	1.89	496	948	3.20:	3.10:
J943A.....	...	0.873[a]	0.976[a]	4980	...	...	214	346	3.40	3.11
J943B.....	...	0.873[a]	0.976[a]	4820	...	...	162	384	3.40	3.17
J968.....	11.6	1.028	1.291	4289:	0.83	1.68	468	566	3.23:	3.13:
J971.....	0.8	1.049	1.363	4194:	0.69	2.31	512	508	2.97:	2.88:
J1017	0.2	1.047	1.172	4466	1.03	1.78	486	474	3.23	3.13
J1036	1.3	1.221	1.593	4035:	0.49	2.20	382	377	2.35:	2.38:
J1037	1.4	1.252	1.563	4022	0.66	1.29	549	553	2.93	2.84
J1077	Abs.	0.705	0.821	5390:	1.68	2.06	282	270	3.38:	3.11:
J1122	27.1	0.685	1.080	4653:	1.25	2.70	487	645	3.98:	3.83:
J1146	0.1	0.873	1.036	4747:	1.36	2.12	431	418	3.47:	3.27:
J1185	0.4	1.007	1.156	4528	1.08	1.62	484	466	3.30	3.20
J1197	0.4	1.115	1.327	4273	0.82	1.52	485	475	2.95	2.86
Nonmembers										
J442.....	ET, abs.	...	1.420[b]	...	...	...	...	...	...	...
J542.....	ET, abs.	1.204	1.596	...	...	...	...	...	...	...
J611.....	Abs.	0.845	0.918	5017	...	...	$\lesssim$14	$\lesssim$14	$\lesssim$0.85	$\lesssim$1.14
J641.....	ET, abs.	...	1.401[b]	...	...	...	...	...	...	...
J779.....	Abs.	0.976	1.064	4657	...	...	$\lesssim$12	$\lesssim$12	$\lesssim$0.33	$\lesssim$0.62
J1088	Abs.	0.617	0.623	5916	...	...	127	127	2.97	2.89
J1302	ET, abs.	...	1.567[b]	...	...	...	...	...	...	...
J1328	ET, abs.	1.111	1.474	...	...	...	...	...	...	...

Note—Entries with colons indicate more uncertain values. An "ET" in col. (2) indicates a probable early-type object.

[a] Photometry is for A and B combined.

[b] Photometry is from R. Makidon (1997, private communication).

tions are much less than the Li line strength. A more important correction is needed for spectrum veiling, and to do this we used the relationship between Hα emission and veiling of Hartmann & Kenyon (1990) as presented by Strom et al. (1989b). The Hα equivalent widths are listed in column (2) of Table 3.

Using these corrected equivalent widths, we calculated Li abundances using the curves of growth tabulated in Paper III. These LTE abundances are then on the same scale as those for other clusters from papers in the present series. Randich et al. (1997) also used these curves of growth for IC 2602. We also determined non-LTE corrections using the code of Carlsson et al. (1994) for [Fe/H] = 0.0 and log g = 3.8. The Carlsson et al. corrections do not extend below $T_{\rm eff}$ = 4500 K, so we used the 4500 K corrections for those cooler stars. Figure 4 of Pavlenko et al. (1995) suggests that this approximation should produce relative Li abundances good to about 0.1 dex. Our estimates of non-LTE Li abundances are given in the last column of Table 3.

Only one of our stars, J943 (W134), has been previously observed for Li. Padgett & Stapelfeldt (1994) measured equivalent widths of 200 and 170 mÅ for the two components of this SB2, whereas we measure 214 and 162 mÅ. (These values are after correction for spectrum veiling, but not for line dilution by the companion.) For J943, an average $T_{\rm eff}$ for the two components was determined from the composite photometry; these were then adjusted by $\pm$80 K so that the final $T_{\rm eff}$ values differed by the 160 K found by Padgett & Stapelfeldt (1994); this difference is consistent with our spectrum as well. The raw (measured) equivalent widths for the Li feature were corrected for flux dilution using the Planck function ratio at 6708 Å for these two $T_{\rm eff}$ values and the relative radii for 3 Myr–old stars

with $Y = 0.28$ and $Z = 0.02$ from D'Antona & Mazzitelli (1997). Our raw and corrected equivalent widths agree well with those reported by Padgett & Stapelfeldt (1994), but our Li abundances are much lower than theirs because of our lower $T_{\rm eff}$ values.

3.4. *Spectroscopic Indicators of Membership*

Our final assessment of membership is given in column (11) of Table 2, and it is based on the original proper-motion estimates, together with spectroscopic indicators. As we noted above, J442, J542, J641, J1302, and J1328 have high proper-motion membership probabilities, but they also show very broad Hα wings, broad and shallow IRT profiles, and no other discernible spectroscopic features except for several diffuse interstellar bands. These five stars most likely lie beyond NGC 2264 and are heavily reddened.

J611 and J779 show Hα absorption and no detectable Li, and they also have low proper-motion membership probabilities and low radial velocities and lie away from cluster members in the color-magnitude diagram (CMD), shown below. They are surely nonmembers.

Membership for J1077 and J1088 is ambiguous. Both show Hα in absorption, but that is also the case for other relatively hot and massive stars in NGC 2264 (King 1993). Both stars have low $v_{\rm rad}$, but that could be due to their being binaries (J1077 is classified as a possible SB2). Both stars have high proper-motion membership probabilities. The Li abundance of J1077 is comparable to that of other hot cluster members, but Li in J1088 is lower than for other stars of similar color in NGC 2264. Also, J1088 is located near the 14 Myr isochrone in the CMD, while more certain members lie between the 1 and 5 Myr isochrones. For the present, we take J1077 to be a probable cluster member and J1088 to be a probable nonmember.

The rest of our sample are all likely to be cluster members on all grounds: proper motions, Hα emission, Li abundance, and position in the CMD. In those cases where the $v_{\rm rad}$ is discrepant, we have assigned them probable membership. In five of these cases (J236, J606, J1036, J1146, and J1185), the CCFs suggest multiplicity.

4. DISCUSSION

4.1. *The Ages of NGC 2264*

Figure 5 shows an H-R diagram for NGC 2264. The corrections to convert M_V to $M_{\rm bol}$ are from Bessell (1991). The evolutionary tracks are from Siess, Forestini, & Dougados (1997) for solar metallicity (Anders & Grevesse 1989). The convergence of the isochrones at low masses arises from deuterium burning, which slows the contraction of the stars.

Most of our stars lie between the isochrones for 1 and 5 Myr. This is consistent with the age estimate of R. Makidon (1997, private communication), 3 Myr, and also the 0.8–8 Myr range seen by SBL. The few stars that lie near or below the 10 Myr isochrone are all probable nonmembers on a variety of grounds (see above). Therefore, we estimate the age spread in NGC 2264 to be only about 4 Myr, about a factor of 2 less than that seen by Adams, Strom, & Strom (1983) and SBL. The better discrimination of membership that spectroscopy affords allows for a better determination of age and age spread. Because star formation is still taking place in NGC 2264 (Margulis et al. 1989), 4 Myr is just a lower bound to the age spread.

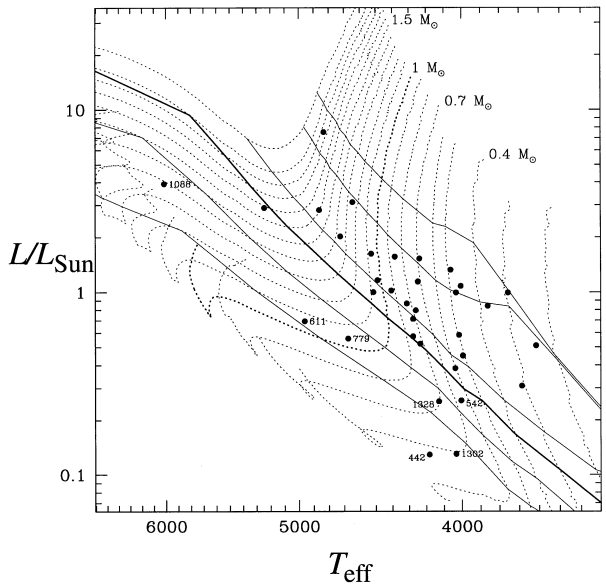

FIG. 5.—H-R diagram for NGC 2264. The dotted lines are mass tracks, with the coolest one corresponding to 0.2 $M_\odot$. The next is for 0.3, then 0.4, 0.55, 0.6 $M_\odot$, and then in increments of 0.10 $M_\odot$ up to 2.0 $M_\odot$, with the last track being for 2.2 $M_\odot$. The solid lines are isochrones, which are, from top to bottom, for 0.5, 1, 3, 5, 10, and 20 Myr. The stars below the 5 Myr isochrone are identified by their J numbers.

The least massive stars tend to appear to be younger than more massive stars. We suspect that this is an artifact of the models because different evolutionary tracks from the literature are especially discrepant below $\sim 0.5\ M_\odot$ (Siess et al. 1997), as a result of differing treatment of the equation of state and electronic corrections in cool degenerate matter. Modeling of the atmosphere also plays a role. This mass-dependent age discrepancy was noted by SBL and is also seen in the Orion Nebula cluster (Hillenbrand 1997).

4.2. *Pre–Main-Sequence Evolution of Angular Momentum*

In addition to the v sin i values reported here, measurements of rotation periods exist for many stars in NGC 2264. We first compare NGC 2264 with the very young (~ 1 Myr old) stars of the Orion Nebula cluster (ONC). Figure 6 shows histograms of rotation periods for NGC 2264 (Kearns et al. 1997; Kearns & Herbst 1998; R. Makidon 1997, private communication) and the ONC (Hillenbrand 1997). Both the ONC and NGC 2264 have distributions with low-$P_{\rm rot}$ peaks and extended tails, but the ONC distribution is distinctly bimodal. Kearns et al. (1997) have already compared ONC with NGC 2264, and they concluded that the moderate rotators in the ONC ($P_{\rm rot} = 6$–10 days) will have spun up to $P_{\rm rot} = 5$ days by the age of NGC 2264. Within the framework of current models, this means that the stars in NGC 2264 have been decoupled from their circumstellar disks for some time. Assuming conservation of angular momentum and taking into account stellar structural changes, a 1 $M_\odot$ star with $P_{\rm rot} = 8$ days will spin up to a period of 3.5, 4.7, or 5.7 days at the age of NGC 2264 if star-disk coupling ceases at an age of 1.0, 1.5, or 2.0 Myr, respectively. These simulations suggest disk-locking timescales of only 1–2 Myr to reproduce the peak at a 5 day period. Observations of infrared excess (Strom et al. 1989a), on the other hand, indicate that disks can last as long as ~ 10 Myr.

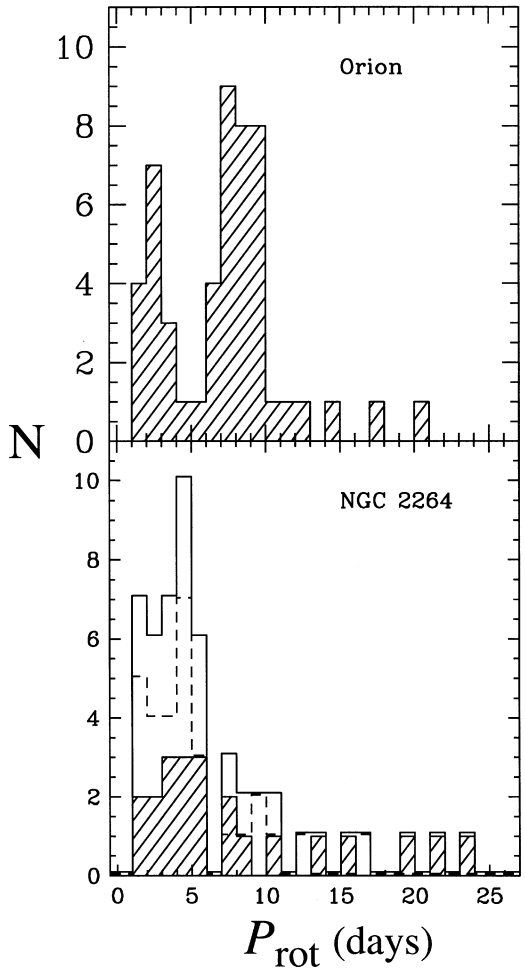

FIG. 6.—Histograms of rotation periods for NGC 2264 and the ONC. In the lower panel, the hatched histogram is for NGC 2264, the dashed histogram is for the ONC (from Kearns & Herbst 1998), and the solid histogram represents the cumulative distribution.

The slow rotators ($P_{rot} \gtrsim 7$ days) in NGC 2264 may be stars that are still coupled to their disks. There is nothing about the positions of the slow rotators in the H-R diagram to indicate that they are systematically younger than the rapid rotators, and so a range of disk lifetimes may be possible.

What happens next? Can the stars of NGC 2264 plausibly evolve into what is seen in the Pleiades or in α Per? We explore two possibilities: solid-body rotation and core-envelope decoupling (angular momentum conservation in shells). In the solid-body case, we presume braking via a stellar wind, using Kawaler's (1998) formulation. In those models, Ω_{crit} represents the critical rotation rate above which the magnetic field saturates; below Ω_{crit} we have $B \propto \Omega$. For core-envelope decoupling, we use τ_{coupl} to denote the timescale for transporting angular momentum from the rapidly rotating core to the convective envelope (MacGregor & Brenner 1991). Angular momentum loss from the envelope is treated the same as for the solid-body case.

For both cases, we assume that the stars are decoupled from their accretion disks (Siess & Livio 1997 present further details of this model). We use the observed P_{rot} values and take NGC 2264 to be 3 Myr old. We take $\tau_{coupl} = 20$ Myr and $\Omega_{crit} = 10\ \Omega_{\odot}$, both of which are in accord with observations.

The angular momentum evolution of stars in the mass range $0.5\ M_{\odot} < M \leq 1.1\ M_{\odot}$ is then followed adopting the two hypotheses. As pointed out by Siess & Livio (1997), both the solid and decoupling models cannot easily reproduce the proportion of very slow rotators ($v \sin i < 10$ km s^{-1}) at the age of α Per and the Pleiades unless "extreme" values of the parameters are used. The solid rotation model requires very long star-disk coupling timescales of the order of 10 Myr (e.g., Bouvier, Forestini, & Allain 1997) to prevent the star from spinning up, while the decoupling model necessitates a very long coupling timescale ($\tau_{coupl} \sim$ 100 Myr) or a high value of Ω_{sat} (e.g., Keppens, MacGregor, & Charbonneau 1995; Allain 1998). Considering the inability of theoretical models to reproduce the proportion of very slow rotators, we did not account for them in our comparisons.

The results of the simulations (Fig. 7) indicate that at the age of α Per (50 Myr), only the decoupling model is able to reproduce the faster rotators with $v \sin i > 100$ km s^{-1}. At the age of the Pleiades (70 Myr), braking has efficiently spun down the stars that are now rotating slowly in both models ($v \sin i < 40$ km s^{-1}). We note, however, that the decoupling model provides a more efficient braking, because only the surface layers of the star are spun down. To compare the different distributions, we performed a χ^2 test. The numbers indicated in Figure 7 suggest that the decoupling hypothesis can better account for the evolution of the periods distribution in NGC 2264.

To conclude this section, the rotation period distribution of NGC 2264 can reasonably be understood as the evolved distribution of younger stars such as in the ONC. Our calculations of the expected distribution of periods at the age of α Per and the Pleiades seem to favor the decoupling model over the solid rotation hypothesis, especially because the former can reproduce the faster rotators. But, considering the small sample, this preliminary conclusion definitely requires additional observations to be confirmed.

4.3. Li *Abundances in NGC 2264*

Nearly all young clusters (ages less than 250 Myr; see Table 1 for references) show a spread in Li abundance for stars with $M \lesssim 1\ M_{\odot}$, but also a generally decreasing Li abundance with decreasing stellar mass. NGC 2264 is young enough that little Li depletion should have taken place. Figure 8 shows the NGC 2264 non-LTE Li abundances as a function of T_{eff}. We have added the observations of King to our sample. The dashed lines in Figure 8 are predicted curves for Li abundance from standard models for 3 (*top*), 10 (*middle*), and 30 Myr (*bottom*) for an initial abundance of log N(Li) = 3.2. The slight downturn in Li abundance in Figure 8 is consistent with standard models and an age for the cluster of slightly more than 3 Myr. The solid lines show where stars would fall if all stars had the same Li abundance of log N(Li) = 3.2 but the derived temperatures were uniformly raised by 250 K (*top line*) or decreased by 250 K (*bottom line*).

Figure 8 shows a substantial overall spread in Li. The range is approximately 0.5 dex in the non-LTE abundances. This is nearly the same spread seen for $\sim 1\ M_{\odot}$ stars in the Pleiades (Paper III), and it is tempting to speculate that the spread we see in the Pleiades is already in place at this early age. However, we do not think this is the case, for several

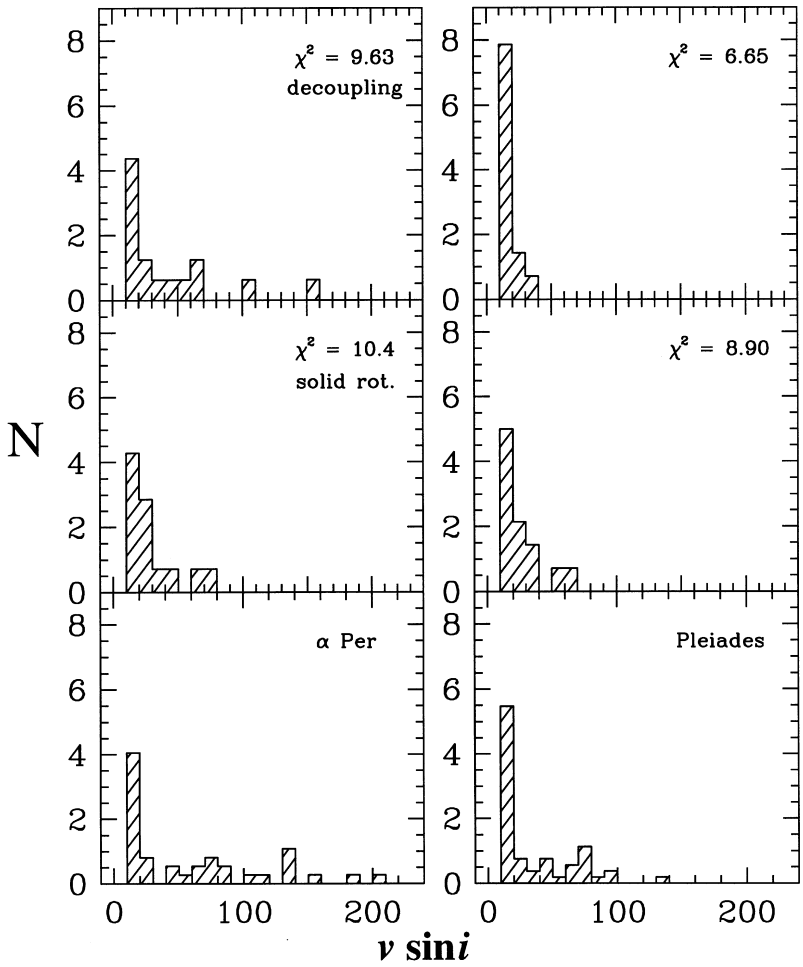

FIG. 7.—Histograms of v sin i as observed in α Per and the Pleiades (*bottom*) and as predicted by models with core-envelope decoupling (*top*) and solid-body rotation (*middle*). The sources of the observations are listed in Soderblom et al. (1993e).

reasons. Foremost is the difficulty in determining temperatures for these stars. From the discussion above, random errors of 250 K (from nonuniform reddening, for example) cannot be ruled out, and errors of this magnitude could account for most of the spread seen for temperatures above 4000 K. There is also the problem of correcting for veiling, and the star with the highest Li abundance is also one of the stars with a large correction. Moreover, if the spread seen is real, than NGC 2264 will be very peculiar at the age of the Pleiades. This is because stars with current temperatures greater than 4500 K will reach the main sequence with temperatures greater than 6000 K. If the current spread is real, then the future NGC 2264 will have a large spread in Li abundance, whereas all other clusters have essentially no spread at this temperature. On theoretical grounds, standard models would predict little or no depletion for nonrotating models, and if the spread seen in Figure 8 were real, it would imply that the spread existed in the proto-nebula of each star.

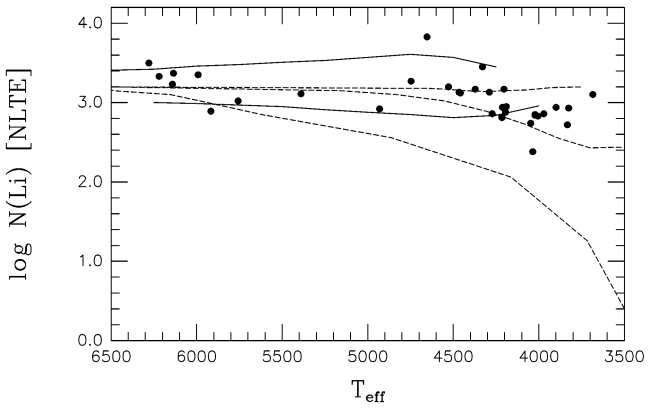

FIG. 8.—log N(Li) vs. $T_{\rm eff}$ for stars in NGC 2264. The dashed lines show standard (nonrotating) models of Li depletion for 3, 10, and 30 Myr (*top to bottom*). The solid lines show the effect of assuming all stars have log N(Li) = 3.2 but with uncertainty in $T_{\rm eff}$ of +250 (*upper line*) and −250 K (*lower line*).

In Paper III we noted that the most Li-rich stars of the Pleiades tended to be ultrafast rotators, as also observed by Butler et al. (1987) and García López et al. (1994). Although this correlation does not extend to cooler Pleiades (Paper VI; García López et al. 1994), other clusters, such as NGC 1039 (Jones et al. 1997, hereafter Paper VII) and α Per (Randich et al. 1998), do show a correlation in the same temperature range as does the Pleiades. Chaboyer et al. (1995) and Martín & Claret (1996) have proposed a solution to account for the connection. However, the situation is complicated by more recent determinations of $P_{\rm rot}$ for the Pleiades (Krishnamurthi et al. 1997) that show that at least one Li-rich star rotates slowly.

Figure 9 shows log N(Li) versus $P_{\rm rot}$ for our NGC 2264 stars. The few Li-rich stars [log N(Li) ≈ 3.5] with very

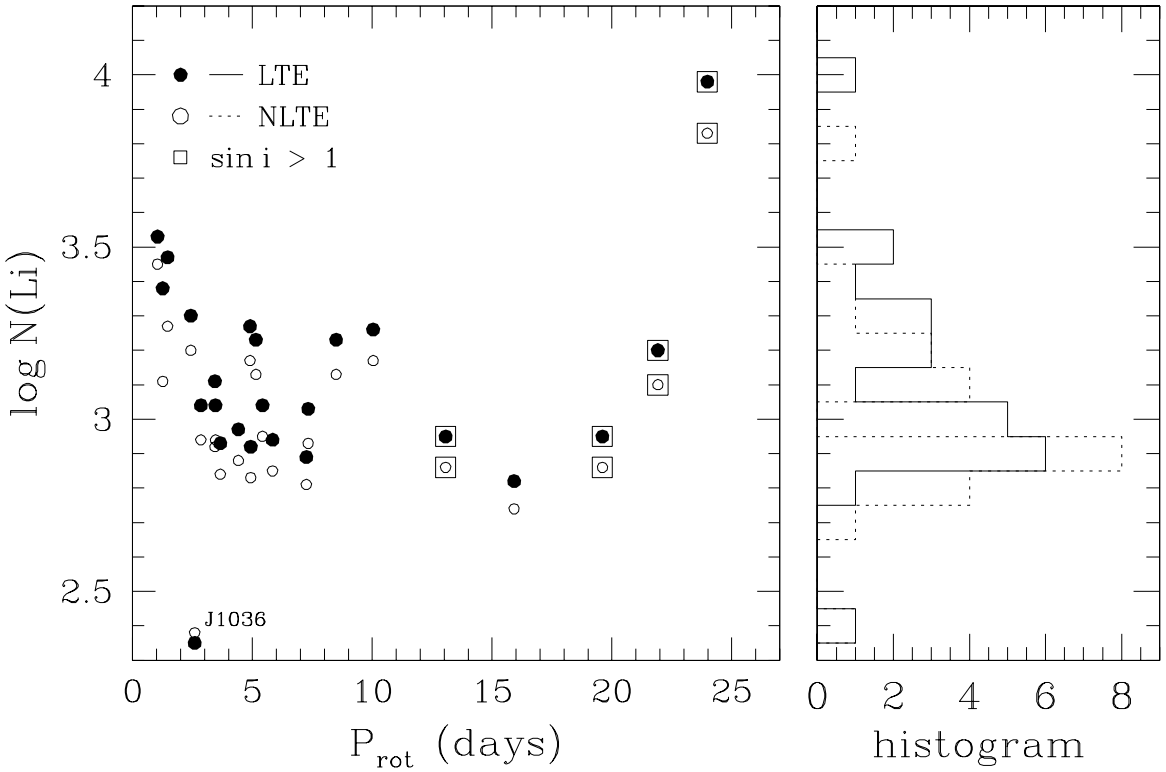

FIG. 9.—*Left*, log N(Li) vs. P_{rot} for stars in NGC 2264; *right*, histograms corresponding to the LTE (*solid line*) and non-LTE (*dotted line*) abundances

small rotation periods are from the high-mass end of our sample, where we expect to see more rapid rotation, and so we conclude that there is no apparent connection between Li abundance and rotation for NGC 2264, as expected from the above discussion. We conclude that the spread in Li abundances seen in the Pleiades arose after an age of 3–5 Myr.

The Li abundances we see in NGC 2264 are consistent with those seen, for instance, in Orion Ic (King 1993), once allowance for non-LTE effects is made in King's data. The non-LTE Li abundances of Cunha, Smith, & Lambert (1995) are also consistent with a uniform value of Li in PMS stars.

4.4. *The Distribution of Rotation Axes*

We have sufficient information to perform a consistency check on the PMS models used here and some measured parameters. We have observed values of P_{rot} and $v \sin i$, plus model-dependent estimates of R, the radii of the stars. Putting these together yields values of sin i:

$$\sin i = P_{rot}(v \sin i)/2\pi R \ .$$

Individual values of sin i are not especially useful, but we can test to see whether the overall distribution of sin i corresponds to a random distribution of rotation axes (Chandrasekhar & Munch 1950), and we also expect that sin i should not exceed 1, except to a minor degree due to uncertainty.

Figure 10 shows our sin i distribution, and it is not as expected. First, there are three stars with sin i much greater than 1. Possibly the v sin i values are too large because these stars are SB2's with blended lines. Alternatively, P_{rot} may be overestimated if aliasing of the period goes undetected. This would require the true rotation period to be half the observed period, which seems unlikely unless the observers were unusually unlucky, although it is suggestive that the stars with sin $i > 1$ all have long rotation periods (Fig. 9). The final possibility is that the radius used is too small, but R is unlikely to be in error by as much as the factor of 2.6 needed to explain the sin i seen for J1122, for example.

Aside from the three cases for which sin i is too large, the average sin i is about 0.6, much lower than expected. For a random distribution of rotation axes, $\langle \sin i \rangle = \pi/4 = 0.79$ (Chandrasekhar & Munch 1950). Except for occasional problems with line blending, v sin i values above 10 km s^{-1} should be reliable to about 10%. As mentioned, P_{rot} can sometimes be off by a factor of 2 because of aliasing,

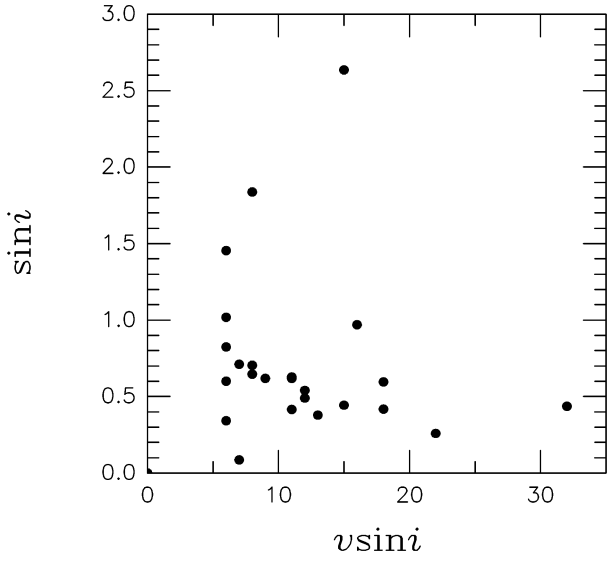

FIG. 10.—Plot of sin i vs. v sin i for stars in NGC 2264

depending on the sampling during the observations, but raising a significant number of sin i values by a factor of 2 puts them above 1, which is unacceptable.

Several other possibilities for the distribution seen in Figure 10 suggest themselves. First, the luminosities and/or effective temperatures of these stars could be systematically overestimated, leading to a shift to higher mass tracks and thus larger estimated radii. Second, we may have missed stars nearly equator-on if they still have accretion disks or other obscuring material. Third, perhaps rotation axes in NGC 2264 tend to be aligned instead of randomly oriented.

Models of PMS stars continue to be refined, of course, but they are internally consistent and have been successful in accounting for much of the observations. In other words, there is no strong evidence for a fundamental problem with them. The presence of circumstellar material around stars as young as those in NGC 2264 is plausible, although it is not thought to be thick or extensive. Finally, other clusters, as well as field stars, have rotation rates that agree with the assumption of randomly distributed axes, so there is little basis for believing NGC 2264 to have some systematic alignment.

The answer to this problem is not clear, but we note that Weaver (1987) saw a very similar distribution of axial inclinations in considering T Tauri stars. Weaver attributed the distribution to selection against high-inclination stars because of circumstellar material.

5. CONCLUSIONS

We have reported on high-resolution echelle spectra of stars in the PMS open cluster NGC 2264. All of our stars that lie below the 5 Myr isochrone are probably nonmembers, and therefore the age spread seen in NGC 2264 is only about 4 Myr. This is substantially less than other determinations, but it is a lower bound because star formation is still taking place in this cluster.

We compared rotation in NGC 2264 members with the even younger ONC and the ZAMS clusters α Per and the Pleiades. Current models can satisfactorily evolve the distribution of rotation seen in the ONC into that seen in NGC 2264. In examining the evolution of rotation to the ZAMS, we considered models with solid-body rotation and with decoupling of the radiative core from the convective envelope. The latter case, with decoupling, appears to fit the observations better.

Because of substantial (250 K) uncertainty in effective temperatures in PMS clusters (because of uneven reddening, among other things), the distribution of lithium abundances seen in NGC 2264 has scatter, but it is consistent with uniform abundances among the members and with no depletion having yet taken place. This suggests that the large spread in Li seen among solar-type stars in the Pleiades and other young clusters arises after an age of at least 3–5 Myr.

We gratefully acknowledge the assistance provided by Russ Makidon in providing observations prior to publication. This work was supported, in part, by NASA grant NAGW-4837 to D. R. S.; B. F. J. acknowledges partial support from NASA grant NAG 5-4830 and NSF grant AST 95-30632. This research has made use of the SIMBAD database, operated at CDS, Strasbourg, France.

REFERENCES

Adams, F. C., Strom, K. M., & Strom, S. E. 1983, ApJS, 53, 893
Allain, S. 1998, A&A, 333, 629
Anders, E., & Grevesse, N. 1989, Geochim. Cosmochim. Acta, 53, 197
Balachandran, S., Lambert, D. L., & Stauffer, J. R. 1988, ApJ, 333, 267 (erratum 470, 1243 [1996])
Bessell, M. S. 1979, PASP, 91, 589
———. 1991, AJ, 101, 662
Boesgaard, A. M., & Budge, K. G. 1988, ApJ, 332, 410
Boesgaard, A. M., Budge, K. G., & Ramsay, M. E. 1988, ApJ, 327, 389
Boesgaard, A. M., & Tripicco, M. J. 1986, ApJ, 302, L49
Bouvier, J., Forestini, M., & Allain, S. 1997, A&A, 326, 1023
Butler, R. P., Cohen, R., Duncan, D. K., & Marcy, G. W. 1987, ApJ, 319, L19
Cameron, L. M. 1985, A&A, 147, 39
Carlsson, M., Rutten, R. J., Bruls, J. H. M. J., & Shchukina, N. G. 1994, A&A, 288, 860
Cayrel, R., Cayrel de Strobel, G., Campbell, B., & Däppen, W. 1984, ApJ, 283, 205
Chaboyer, B., Demarque, P., & Pinsonneault, M. H. 1995, ApJ, 441, 876
Chandrasekhar, S., & Munch, G. 1950, ApJ, 111, 142
Cunha, K., Smith, V. V., & Lambert, D. L. 1995, ApJ, 452, 634
D'Antona, F., & Mazzitelli, I. 1997, Mem. Soc. Astron. Italiana, 68, 807
Duncan, D. K., & Rebull, L. M. 1996, PASP, 108, 738
García López, R. J., Rebolo R., & Beckman, J. E. 1988, PASP, 100, 1489
García López, R. J., Rebolo R., & Martín, E. L. 1994, A&A, 282, 518
Hartmann, L. W., & Kenyon, S. J. 1990, ApJ, 349, 190
Herbig, G. H., & Leka, K. D. 1991, ApJ, 382, 193
Hillenbrand, L. A. 1997, AJ, 113, 1733
Hobbs, L. M., & Pilachowski, C. 1986a, ApJ, 309, L17
———. 1986b, ApJ, 311, L37
———. 1988, ApJ, 334, 734
James, D. J., & Jeffries, R. D. 1997, MNRAS, 292, 252
Jeffries, R. D. 1997, MNRAS, 292, 177
Jeffries, R. D., James, D. J., & Thurston, M. R. 1998, MNRAS, 300, 550
Jones, B. F. 1999, in preparation
Jones, B. F., Fischer, D., Shetrone, M., & Soderblom, D. R. 1997, AJ, 114, 352 (Paper VII)
Jones, B. F., Fischer, D., & Soderblom, D. R. 1999, AJ, 117, 330 (Paper VIII)
Jones, B. F., Shetrone, M., Fischer, D., & Soderblom, D. R. 1996, AJ, 112, 186 (Paper VI)
Kawaler, S. D. 1988, ApJ, 333, 236
Kearns, K. E., Eaton, N. L., Herbst, W., & Mazzurco, C. J. 1997, AJ, 114, 1098
Kearns, K. E., & Herbst, W. 1998, AJ, 116, 261
Keppens, R., MacGregor, K. B., & Charbonneau, P. 1995, A&A, 294, 469
King, J. R. 1993, AJ, 105, 1087
———. 1998, AJ, 116, 254
Krishnamurthi, A., Pinsonneault, M. H., Barnes, S., & Sofia, S. 1997, ApJ, 480, 303
Lang, K. R. 1992, Astrophysical Data: Planets and Stars (New York: Springer)
Liu, T., Janes, K. A., & Bania, T. M. 1989, AJ, 98, 626
MacGregor, K. B., & Brenner, M. 1991, ApJ, 376, 204
Makidon, R. B., Strom, S. E., Tingley, B., Adams, M. T., Hillenbrand, L., Hartmann, L. W., Calvet, N., & Jones, B. F. 1997, BAAS, 191, No. 5.06
Margulis, M., Lada, C. J., & Young, E. T. 1989, ApJ, 345, 906
Martín, E. L., & Claret, A. 1996, A&A, 306, 408
Martín, E. L., & Montes, D. 1997, A&A, 318, 805
Meynet, G., Mermilliod, J.-C., & Maeder, A. 1993, A&AS, 98, 477
Padgett, D. L. 1996, ApJ, 471, 847
Padgett, D. L., & Stapelfeldt, K. R. 1994, AJ, 107, 720
Panagi, P. M., O'Dell, M. A., Cameron, A. C., & Robinson, R. D. 1994, A&A, 292, 439
Pasquini, L., Randich, S., & Pallavicini, R. 1997, A&A, 325, 535
Pavlenko, Y. V., Rebolo, R., Martín, E. L., & García López, R. J. 1995, A&A, 303, 807
Pérez, M. R., Thé, P. S., & Westerlund, B. E. 1987, PASP, 99, 1050
Pilachowski, C., & Hobbs, L. M. 1988, PASP, 100, 336
Randich, S., Aharpour, N., Pallavicini, R., Prosser, C. F., & Stauffer, J. R. 1997, A&A, 323, 86
Randich, S., Martín, E. L., García López, R. J., & Pallavicini, R. 1998, A&A, 333, 591
Russell, S. C. 1996, ApJ, 463, 593
Siess, L., Forestini, M., & Dougados, C. 1997, A&A, 324, 556
Siess, L., & Livio, M. 1997, ApJ, 490, 785
Soderblom, D. R., Fedele, S. B., Jones, B. F., Stauffer, J. R., & Prosser, C. F. 1993a, AJ, 106, 1080 (erratum 109, 1402 [1995]) (Paper IV)
Soderblom, D. R., Jones, B. F., Balachandran, S., Stauffer, J. R., Duncan, D. K., Fedele, S. B., & Hudon, J. D. 1993b, AJ, 106, 1059 (Paper III)
Soderblom, D. R., Jones, B. F., Stauffer, J. R., & Chaboyer, B. 1995, AJ, 110, 729 (Paper V)
Soderblom, D. R., Oey, M. S., Johnson, D. R. H., & Stone, R. P. S. 1990, AJ, 99, 595 (Paper I)

Soderblom, D. R., Pilachowski, C., Fedele, S. B., & Jones, B. F. 1993c, AJ, 105, 2299 (Paper II)
Soderblom, D.R., Stauffer, J. R., Hudon, J. D., & Jones, B. F. 1993d, ApJS, 85, 315 (SSHJ)
Soderblom, D. R., Stauffer, J. R., MacGregor, K. B., & Jones, B. F. 1993e, ApJ, 409, 624
Spite, F., Spite, M., Peterson, R. C., & Chaffee, F. H. 1987, A&A, 171, L8
Stauffer, J. R., Hartmann, L. W., Jones, B. J., & McNamara, B. R. 1989, ApJ, 342, 285
Strom, K. M., Strom, S. E., Edwards, S., Cabrit, S., & Skrutskie, M. F. 1989a, AJ, 97, 1451
Strom, K. M., Wilkin, F. P., Strom, S. E., & Seaman, R. L. 1989b, AJ, 98, 1444
Sung, H., Bessell, M. S., & Lee, S.-W. 1997, AJ, 114, 2644 (SBL)
Thorburn, J. A., Hobbs, L. M., Deliyannis, C. P., & Pinsonneault, M. H. 1993, ApJ, 415, 150
Vasilevskis, S., Sanders, W. L., & Balz, A. G. A., Jr. 1965, AJ, 70, 797
Vogt, S. S. 1992, in ESO Workshop on High Resolution Spectroscopy with the VLT, ed. M.-H. Ulrich (Garching-ESO), 223
Walker, M. F. 1956, ApJS, 2, 365
Weaver, W. B. 1987, ApJ, 319, L89